UNIVERSITÉ DE GENÈVE

Archive ouverte UNIGE
https://archive-ouverte.unige.ch

Article scientifique | Article | 2014

Accepted version | Open Access

This is an author manuscript post-peer-reviewing (accepted version) of the original publication. The layout of the published version may differ .

Short-term acclimation of the photosynthetic electron transfer chain to changing light: a mathematical model

Ebenhöh, Oliver; Fucile, Geoffrey; Finazzi, Giovanni; Rochaix, Jean-David; Goldschmidt-Clermont, Michel P.

How to cite

EBENHÖH, Oliver et al. Short-term acclimation of the photosynthetic electron transfer chain to changing light: a mathematical model. In: Philosophical transactions - Royal Society. Biological sciences, 2014, vol. 369, n° 1640, p. 20130223. doi: 10.1098/rstb.2013.0223

This publication URL: https://archive-ouverte.unige.ch/unige:36561
Publication DOI: 10.1098/rstb.2013.0223

© This document is protected by copyright. Please refer to copyright holder(s) for terms of use.

"Short-term acclimation of the photosynthetic electron transfer chain to changing light: a mathematical model"

Oliver Ebenhöh[1,2,†], Geoffrey Fucile[3,†], Giovanni Finazzi[4,5,6,7], Jean-David Rochaix[3], Michel Goldschmidt-Clermont[3,*]

[1]University of Aberdeen, Institute for Complex Systems and Mathematical Biology, Meston Building, Old Aberdeen, Aberdeen AB24 3UE

[2]GFZ German Research Centre for Geosciences, Section 4.5 Geomicrobiology, Telegrafenberg, 14473 Potsdam, Germany

[3]Department of Botany and Plant Biology and Department of Molecular Biology, University of Geneva, 30 quai Ernest Ansermet, 1211 Geneva 4, Switzerland

[4]Centre National de la Recherche Scientifique, Laboratoire de Physiologie Cellulaire & Végétale, Unité Mixte de Recherche 5168, F-38054 Grenoble, France

[5]Université Grenoble-Alpes, F-38054 Grenoble, France

[6]Commissariat à l'Energie Atomique et Energies Alternatives, Institut de Recherches en Technologies et Sciences pour le Vivant, F-38054 Grenoble, France

[7]Institut National Recherche Agronomique, Unité Sous Contrat 1359, F-38054 Grenoble, France

[†] These authors contributed equally to this work
[*] Author for correspondence (Michel.Goldschmidt-Clermont@unige.ch)

ABSTRACT

Photosynthetic eukaryotes house two photosystems with distinct light absorption spectra. Natural fluctuations in light quality and quantity can lead to unbalanced or excess excitation, compromising photosynthetic efficiency and causing photodamage. Consequently, these organisms have acquired several distinct adaptive mechanisms, collectively referred to as non-photochemical quenching of chlorophyll fluorescence (NPQ), which modulate the organization and function of the photosynthetic apparatus. The ability to monitor NPQ processes fluorometrically has led to substantial progress in elucidating the underlying molecular mechanisms. However, the relative contribution of distinct NPQ mechanisms to variable light conditions in different photosynthetic eukaryotes remains unclear. Here we present a mathematical model of the dynamic regulation of eukaryotic photosynthesis using ordinary differential equations. We demonstrate that, for Chlamydomonas, our model recapitulates the basic fluorescence features of short-term light acclimation known as state transitions, and discuss how the model can be iteratively refined by comparison with physiological experiments to further our understanding of light acclimation in different species.

Keywords: photosynthesis, light acclimation, state transitions, non-photochemical quenching, *Chlamydomonas reinhardtii*, mathematical modeling

INTRODUCTION

The light-dependent electron transfer reactions of eukaryotic photosynthesis are catalyzed by serially linked protein complexes within the thylakoid membranes of chloroplasts [1-4]. Linear photosynthetic electron flow (LEF) commences with the light harvesting complex II (LHCII) proteins associated with photosystem II (PSII), which channel light energy to the PSII reaction center that catalyzes oxidation of water to form molecular oxygen and protons in the thylakoid lumen. The electrons derived from PSII water-splitting are transferred through the thylakoid membrane by plastoquinone to the cytochrome *b6f* complex (Cyt*b6f*). The Cyt*b6f* catalyzes the translocation of protons from the thylakoid stroma to lumen while transferring the electrons to PSI via plastocyanin or cytochrome c_6. Light harvesting proteins associated with PSI drive the transfer of these electrons through PSI to ferredoxin, which can subsequently reduce $NADP^+$ to NADPH via ferredoxin-NADP reductase. The proton gradient generated by the activities of PSII and Cyt*b6f* powers ATP synthase-catalysed phosphorylation of ADP. Cyclic electron flow (CEF) involves the flow of electrons from ferredoxin to the plastoquinone pool, resulting in increased acidification of the thylakoid lumen and increased production of ATP at the expense of NADPH [5,6]. A remarkable feature of oxygenic photosynthesis is the extremely wide range of reaction kinetics both within the electron transfer chain and the light-independent reactions of carbon fixation [7]. This is further complicated by the distinct light absorption spectra of PSII and PSI (the latter being excited by longer wavelengths than the former), as unbalanced excitation of the two photosystems can lead to over-reduction (or over-oxidation) of the electron carriers connecting the two photosystems, leading to possible photo-oxidative damage to the cell. To achieve “photostasis” amidst the broad range of light quality and quantity found in nature [7], photosynthetic organisms must balance the harvesting, dissipation, and utilization of light energy [8].

The mechanisms of dynamic light acclimation occur across a wide range of time scales. Long-term responses (LTR) include possible adjustments of photosystem stoichiometries [9] and thylakoid membrane folding [10]. These LTR mechanisms do not require photoreceptors and are thought to be primarily regulated by the thylakoid redox poise which controls retrograde signaling from the chloroplast to the nucleus [11]. Photoreceptor-dependent LTR mechanisms can affect the re-positioning of chloroplasts along light gradients [12,13]. Motile photosynthetic organisms such as Chlamydomonas perceive light via rhodopsins to trigger phototactic responses [14,15]. On shorter time scales, excess energy can be dissipated through the transfer of electrons to O_2 via the plastid terminal oxidase [16-18] or at the PSI acceptor side via the Mehler reaction [19]. However, short-term acclimation processes act primarily at the level of PSII and are collectively referred to as non-photochemical quenching of chlorophyll fluorescence (NPQ) [20,21]. NPQ is defined as the difference between the fluorescence maximum of dark-adapted cells and the fluorescence maximum observed during subsequent illumination [20]. The deconvolution of NPQ into three distinct components qE, qT, and qI can be derived from the relaxation kinetics of NPQ in the dark [22]. The qE component of NPQ operates within seconds to minutes and is regulated by the lumenal pH [23]. Acidification of the thylakoid lumen stimulates xanthophyll de-epoxidation and/or conformational changes of the PSII antennae resulting in the dissipation of excess energy as heat [24,25]. Lumen acidification also directly regulates photosynthetic electron flow by decreasing the rate of plastoquinol oxidation by Cyt*b6f* [26]. The qT component, also referred to as ‘state transition’, operates on the scale of minutes and involves the reversible association of LHCII proteins with PSII and PSI to regulate the relative light absorption cross-section of the two photosystems [27]. The mobilization of LHCII proteins between the photosystems is regulated by antagonistic kinases and phosphatases [28]. The qI component has been ascribed to photoinhibition, wherein photodamaged PSII complexes are partially disassembled and repaired on the scale of hours [29].

Although the molecular mechanisms of light acclimation are becoming clear, the conditions required for their induction and their relative contribution to photostasis across variable light conditions remain poorly understood. Light acclimation processes also differ substantially among photosynthetic species and cell types. For example, PTOX-mediated reduction of O_2 is a minor pathway in land plants but can absorb up to 50% of the electrons derived from water splitting in cyanobacteria and some eukaryotic algae [30,31]. Land plants and algae have distinct molecular mechanisms underlying qE. The PSBS protein is critical for qE in vascular land plants [32] but its role in green algae is unclear [33] and diatoms apparently do not encode this protein [34]. Conversely, the qE mechanism of eukaryotic algae such as Chlamydomonas relies heavily on the LHCSR proteins, which are absent in vascular land plants [34]. State transitions also differ substantially between land plants and algae. Whereas land plants mobilize only 15-20% of the LHCII pool, state transitions in the alga *Chlamydomonas reinhardtii* have been reported to involve up to 80% of the LHCII antennae [36]. Some regulatory features of the LHCII kinase (Stt7/STN7) are shared between algae and land plants, such as its decreased activity under high light stress [37-39] and its activation by the binding of plastoquinol to Cyt*b6f* [40-42]. It is currently unknown whether the LHCII phosphatase PPH1/TAP38 [43,44] is regulated, and specific orthologs have not been characterized outside of the land plant lineage.

The analysis of light acclimation mutants has been useful in identifying distinct molecular mechanisms, however these processes do not operate in isolation and they form an interdependent and complex regulatory network. Indeed, the fine tuning of LEF and CEF also varies substantially across species and cell types, with CEF reaching high rates in bundle sheath cells of C4 leaves whereas CEF rarely exceeds 10% in C3 leaves at steady state [45,46]. The relationship between the rate of CEF and NPQ also remains poorly understood. The processes are evidently linked based on the analysis of mutants which are defective in both processes. For example, mutation of PGR5/PGRL1 in Arabidopsis, two proteins required for the “antimycin A-sensitive” CEF pathway [47], also suppresses qE [48], most likely because of the diminished capacity of lumen acidification in the light. In Chlamydomonas, the analysis of *npq4 stt7* double mutants indicates that qE and qT are functionally linked during high light stress [49]. The qT component has also been linked to the regulation of CEF by the analysis of *stt7* mutants [50,51] and the enrichment of CEF supercomplexes in conditions favoring the association of mobile LHCII antennae with PSI [52,53]. However, this conclusion has been recently questioned by a study demonstrating that although the migration of LHCII antennae to PSI can enhance CEF in light-limiting conditions, Chlamydomonas cells may switch from low to high rates of CEF independently of the LHCII kinase Stt7 [54].

Mathematical modeling is a useful tool for studying the dynamic behaviour of biological networks. Discrepancies between the predictions of a mathematical model and observations from physiological and biochemical experiments represent gaps in our theoretical understanding. The predictive power of the mathematical model can be iteratively refined by exploring its parameter space and connectivity based on comparison with empirical data [55-57]. Here we present a mathematical model describing short-term acclimation of the photosynthetic electron transfer chain to changing light. Most of the initial parameters of the model, including reaction kinetics and the variable connectivity of photosynthetic electron transport, were derived from the literature, and the dynamic processes are represented as ordinary differential equations. We demonstrate that our model can reproduce the basic fluorescence measurements during short-term acclimation under conditions promoting state transitions and discuss how the parameter space of the model can be further refined to improve our understanding of the mechanisms of adaptation to changing light.

METHODS

Experimental

Chlamydomonas reinhardtii cells were grown in acetate medium (TAP) under dim light (10 µE $m^{-2}s^{-1}$ from white fluorescent tubes) at 25°C to a density of $2*10^6$ cells/mL. They were collected by centrifugation and resuspended in minimal medium (HSM) at a density of $2*10^7$ cells/mL and incubated under agitation in dim light for one hour for anoxia-induced state transitions and in complete darkness for one hour for light regime-induced state transitions. Fluorescence traces were recorded with a PAM Fluorescence Monitoring System (Hansatech, UK).

Theoretical

The mathematical model as described below and detailed in the Supplementary Material comprises a set of 7 coupled ordinary differential equations. The equations are presented and explained in detail in the Supplementary Information. The parameters were taken from literature and subsequently adapted to fit the experimental curves. The numerical simulations of the equations were carried out with MATLAB.

RESULTS and DISCUSSION

We have built a mathematical model with the goal to provide a theoretical framework in which short-term acclimation processes can be investigated by computer simulations. The purpose of the model is to verify whether current concepts are sufficient to explain experimental observations, to provide a platform to test mechanistic hypotheses, and to make theoretical predictions about the dynamics of variable quantities which cannot be monitored continuously. The model includes all relevant processes involved in the electron transport chain, but is deliberately kept as simple as possible. We here focus on the investigation of state transitions in the green alga *Chlamydomonas reinhardtii* and thus see our work as a continuation of previous theoretical approaches to study NPQ, which addressed in particular the qE component [58,59].

Our experimental data were obtained for Chlamydomonas cells grown in dim light, which do not express LhcSR3 and have little capacity for qE-dependent quenching [35]. This allowed us in a first step to investigate exclusively the qT component and study its dynamics and regulation. A schematic of the model is presented in Figure 1A. Since the model aims at describing adaptation processes in the time-scale of seconds to minutes, it does not include a detailed description of the internal processes of the photosynthetic complexes, but rather uses a heuristic approach to represent their overall function. Thus, photosystem II (PSII), cytochrome b6f (Cyt*b6f*) and photosystem I (PSI) are treated as oxidoreductases, of which the two photosystems are light-driven. In conjunction, these three complexes mediate linear electron flow from water to ferredoxin. The protons concomitantly translocated from stroma to lumen drive the ATP synthase, generating ATP in the stroma. Electrons from ferredoxin can either be used to produce redox equivalents in the form of NADPH by the enzyme FNR, or re-injected into the plastoquinone (PQ) pool (cyclic electron flow). A central aim of the model is to study state transitions. Therefore, the action of the kinase Stt7 and the phosphatase Pph1 are represented in the model. We chose to make the simplifying assumption that the action of Stt7 directly results in a translocation of antenna from PSII to PSI and that Pph1 mediates the reverse translocation. As a result, the cross-sections of the photosystems change, leading to an altered differential activation. In the

model, the Stt7 kinase is regulated by the redox state of the PQ pool, reflecting the existing experimental evidence [60]. In the current version of the model, we assume that the Pph1 phosphatase is constitutively active.

A minimally invasive way to continuously monitor the state of the electron transport chain is through chlorophyll fluorescence measurements. In order to allow comparison of model predictions with such experimental observations, we need to calculate the fluorescence emitted from PSII. For this, we include in the model a simplified representation of the internal processes in PSII (see Fig. 1B). Again, to keep the model as simple as possible, we exploit the time-scale separation (energy transfer within the photosystems are much faster than electron transfer between the complexes of the transport chain) and treat the internal states of PSII as being approximately in steady state (standard quasi steady-state assumption, see Supplementary Material for details).

State transitions can be induced by altering the redox state of the PQ pool either by changing the illumination state (dark versus light) or through switching between aerobic and anaerobic conditions. Under anaerobic conditions in the dark, mitochondrial respiration is arrested and the demand for ATP induces an increase in glycolysis and an accumulation of reducing equivalents (Pasteur effect) that lead to a reduction of the PQ pool and a transition to State 2 [61]. To calibrate and test the model, we compared the simulations with fluorescence traces for state transitions observed experimentally under these two schemes.

The upper panel of Figure 2 presents experimental data (black) and simulation (grey) for dark-adapted wild-type cells that were illuminated by weak light (100 $\mu Es^{-1}m^{-2}$) for 10 minutes. It can be observed that the key features of the experimental fluorescence signal are correctly reproduced by the simulations. The dynamics of the saturating peaks (F_M') reflect the change in antenna cross-section of PSII. Illumination causes a reduction of the PQ pool (see Supplementary Figure S1), activating the kinase Stt7 and thus a partial transition to state 2. Antenna migration to PSI leads to a weaker activation of PSII and thus a slower reduction of the PQ pool. This negative feedback of the state transitions on PQ reduction leads to the establishment of a stationary and stable redox poise. In darkness, the process slowly reverses towards state 1. The steady-state fluorescence (F_S) in the dark is also very well captured, including the slow fluorescence decline between consecutive peaks caused by re-oxidation of the PQ pool after its transient reduction through the actinic effect of the saturating flashes. The relative F_S levels in the light compared to darkness is not precisely reproduced. Why this is the case needs further exploration, and it is likely that a more detailed model of the internal processes in PSII will be necessary to refine the calculation of the fluorescence signal. However, the important feature, i.e. the tendency of F_S to increase shortly after light exposure and then to decline on a longer time scale as shown in the first studies of state transitions [62], is also clearly visible in the simulation results.

The lower panel of Figure 2 shows experimental data and simulations for state transitions induced by shifting low light-adapted wild-type cells from aerobic to anaerobic conditions and back in darkness. Importantly, the simulations have been performed with exactly the same parameters as were used to fit the curves in the upper panel. Again, the important features of the fluorescence signals are well reproduced by the model. The dynamics of F_M' follow the change in antenna cross-section of PSII while F_S reflects, at least qualitatively, the change of redox state of the PQ pool. Interestingly, the inter-flash dynamics of F_S again are reproduced with remarkable accuracy. While in the beginning of the anoxic period, F_S remains approximately constant between two consecutive flashes, later in that phase it exhibits a slight increase. Investigating the variables which are not directly observable explains this behaviour (Supplementary Figure S2). While the PQ pool gets reduced by electrons from glycolysis, the cross-section of PSII simultaneously decreases. Early during anoxia, these processes proceed with approximately the same rate and the opposite effects on fluorescence cancel each other. Later, state

transition is mostly completed and the reduction in cross-section is slowed, leading to a fluorescence rise resulting from PQ reduction.

The fact that the simulations are in good agreement with the experimental data allows us to conclude that our current knowledge and assumptions about the molecular mechanisms of state transitions in Chlamydomonas are sufficient to reproduce and explain most of the fluorescence changes, which are related to the dynamic allocation of antenna to the two photosystems. However, mathematical models are not only useful to reproduce and explain observed behaviour, but also to make further predictions and attempt to answer more fundamental questions. For example, to address the question why state transitions are more pronounced in low light and seem to be repressed under high light conditions, we employed the model with the parameters used above to systematically analyse the steady-state behaviour for different light intensities and different relative antenna cross-sections. For this, the rate constants for the kinase Stt7 and the phosphatase Pph1 were set to zero and the relative cross-section was fixed to different values. Subsequently, the system was simulated until it reached steady state. Figure 3 displays the computed steady-state redox state of the PQ pool as a function of the relative cross-section and the total light intensity. A remarkable observation is a sharp transition of the PQ redox state for low light intensities. If the cross-section of PSII is too small, the pool is almost completely oxidised, while for too large cross-sections, it is extremely reduced. This illustrates the need to finely adapt the relative antenna cross-section under low light conditions to maintain a redox poise. In contrast, for high-light conditions the transition from oxidised to reduced PQ is much smoother, indicating a higher flexibility with respect to relative cross-sections to maintain a redox poise.

So far we have deliberately excluded the qE component of NPQ, thus mimicking low-light adapted Chlamydonomas cells. With the modelling framework developed here, it is straightforward to include equations representing energy-dependent quenching of chlorophyll fluorescence, which may reflect the situation in high-light adapted Chlamydomonas or plants. In a first approach, we have included a simplified mechanism [58] in which one pH-induced quencher increases the rate of chlorophyll de-excitation. When repeating the steady-state calculation (Supplementary Text and Supplementary Fig. S3), an explanation for the different behaviours in different light regimes can be found. While the presence of qE-dependent quenching does not alter the behaviour for low light, in high light it results in the formation of a plateau, in which the redox state of the PQ pool remains relatively constant for a wide range of relative cross-sections. These theoretical predictions lead us to hypothesize that the intrinsic dynamic properties of the electron transport chain demand the ability to adjust antenna cross-sections, but that this requirement is weaker for high-light conditions. Indeed phosphorylation of the LHCII antenna, which is largely mediated by the STN7/Stt7 kinase in low light, is inhibited at high light intensities [49,63]. This has been ascribed to negative regulation of the kinase through the thioredoxin pathway in high light [37,64] or to a conformational change in the PSII antenna [65].

CONCLUSIONS and PERSPECTIVES

This work further extends previous studies on modelling high light acclimation in plants [58]. Here our aim is to recapitulate the basic fluorescence features of short-term light acclimation in Chlamydomonas known as state transitions, which take place in low light (or in the dark under particular environmental conditions), and which are prominent in *Chlamydomonas reinhardtii*. To do so, we have implemented the representation of the photosynthetic electron transport chain in the model (Fig. 1A). In particular, we have included a heuristic description of cyclic electron flow which enhances the proton gradient and thereby triggers qE. We also have taken into account the chlororespiratory pathway which modulates the redox state of the plastoquinone pool in the dark, thereby activating the Stt7 kinase

under anaerobic conditions (Fig 2B). We have also implemented a mechanistic representation of the PSII catalytic cycle (Fig. 1B), to reproduce the changes of fluorescence yield induced by the saturating pulses, which are used to monitor changes in the PSII absorption cross section in vivo (Fig. 2).

Overall, the fact that key experimental features of fluorescence traces are reproduced by the model with good agreement indicates that our model provides a reliable representation of state transitions in the light, and in the dark upon changes from aerobic to anaerobic conditions, despite the quantitative differences that simulations and experimental data show. This implies that this description of photosynthesis as a global process (from light capture to carbon assimilation) is sufficiently accurate to simulate redox changes in the electron transport chain, which take place either in the light through PSII and PSI photochemistry, or in the dark through metabolic exchanges with the cell cytosol surrounding the chloroplast.

We can foresee several applications for this model, in particular mechanistic issues related to photosynthetic activity. This is exemplified by the finding that, while the overall changes in the PSII absorption cross section in the light are well reproduced by the model, the large reduction of the PQ pool in the light cannot be properly simulated. This could suggest that the model is unable to describe the *in vivo* changes of the redox state of the PQ pool. However, this could also indicate that the "classic" picture of state transitions in Chlamydomonas is not entirely correct. This view assumes that all the light harvesting complexes migrate from PSII to PSI during a transition to state 2. By equilibrating their light harvesting capacity, qT leads to a balance between PSII and PSI, which in our simulations restores the redox poise of the PQ pool between state 1 and state 2 more extensively than in our experiments. On the other hand, previous studies have suggested that a substantial fraction of LHCII detaches from PSII during a transition to state 2, but does not associate to PSI and remains in a quenched state in the thylakoids [52]. In this case, state transitions are not expected to induce a complete redox balance of the PQ pool, because the decreased activity of PSII is not compensated by a concomitant enhancement of PSI activity. Obviously, the model can be used to test this hypothesis. Moreover, our model can bring essential information concerning the physiology of light acclimation by simulating the relative weight of qE and qT under changing light conditions, and therefore allows an exploration of the interplay between the two processes (e.g. [49]) under a wide range of simulated environmental conditions. Eventually, the model opens the possibility to investigate evolutionary issues. For example, it can be used to explore the different qE and qT capacity of plants and algae by modifying the appropriate parameters. It can also be used to understand why other ecologically relevant organisms (like diatoms) have evolved a strong qE response, without any need for qT development in their marine environment (e.g. [66,67]).

ACKNOWLEDGMENTS

M. Goldschmidt-Clermont was supported by the SystemsX.ch RTD "Plant Growth in a Changing Environment" and by the Swiss National Foundation (31003A_146300). O. Ebenhöh, G. Finazzi and M. Goldschmidt-Clermont benefited from the Marie Curie ITN "AccliPhot" (GA 316 427). J-D. Rochaix acknowledges a grant from the Swiss National Foundation (3100A0_117712). G. Fucile was supported by an EMBO Post-Doctoral Fellowship. Mutual visits between Geneva and Aberdeen were funded by the Royal Society through the International Exchanges Grant (Ref IE110263). Giovanni Finazzi acknowledges funding by the French National Foundation Agency (ANR grant phytadapt ANR-NT09_567009), and the Labex GRAL (Grenoble Alliance for Integrated Structural Cell Biology) grants. We thank Nicolas Roggli for preparing the figures.

REFERENCES

[1] Arnon, D.I., Allen, M.B. & Whatley, F.R. 1954 Photosynthesis by isolated chloroplasts. *Nature* **174**, 394-396.

[2] Hill, R. & Bendall, F. 1960 Function of the two cytochrome components in chloroplasts—a working hypothesis. *Nature* **186**, 136–137.

[3] Nelson, N. & Ben-Shem, A. 2004 The complex architecture of oxygenic photosynthesis. *Nat. Rev. Mol. Cell. Biol.* **5**, 971-982.

[4] Dekker, J. P. & Boekema, E. J. 2005 Supramolecular organization of thylakoid membrane proteins in green plants. *Biochim. Biophys. Acta.* **1706**, 12-39.

[5] Fork, D. C. & Herbert, S. K. 1993 Electron transport and photophosphorylation by photosystem I in vivo in plants and cyanobacteria. *Photosynth. Res.* **36**, 149–168.

[6] Munekage, Y., Hashimoto, M., Miyake, C., Tomizawa, K., Endo, T., Tasaka, M., Shikanai T. 2004 Cyclic electron flow around photosystem I is essential for photosynthesis. *Nature* **429**, 579-582.

[7] Hüner, N. P., Bode, R., Dahal, K., Hollis, L., Rosso, D., Krol, M., Ivanov, A. G. 2012 Chloroplast redox imbalance governs phenotypic plasticity: the "grand design of photosynthesis" revisited. *Front. Plant Sci.* **3,** 255.

[8] Eberhard, S., Finazzi, G., Wollman, F.A. 2008 The dynamics of photosynthesis. *Annu. Rev. Genet.* **42**, 463–515.

[9] Bonardi, V., Pesaresi, P., Becker, T., Schleiff, E., Wagner, R., Pfannschmidt, T., Jahns, P., Leister, D. 2005 Photosystem II core phosphorylation and photosynthetic acclimation require two different protein kinases. *Nature* **437**, 1179–1182.

[10] Fristedt, R., Willig, A., Granath, P., Crèvecoeur, M., Rochaix, J. D., Vener, A. V. 2009 Phosphorylation of photosystem II controls functional macroscopic folding of photosynthetic membranes in Arabidopsis. *Plant Cell* **21,** 3950-3964.

[11] Foyer, C. H. & Noctor, G. 2013 Redox signaling in plants. *Antioxid. Redox Signal.* **18**, 2081-2090.

[12] Kasahara, M., Kagawa, T., Oikawa, K., Suetsugu, N., Miyao, M., Wada, M. 2002 Chloroplast avoidance movement reduces photodamage in plants. *Nature* **420**, 829–832.

[13] Wada, M., Kagawa, T., Sato, Y. 2003 Chloroplast movement. *Annu. Rev. Plant Biol.* **54**, 455–468.

[14] Zacks, D. N., Derguini, F., Nakanishi, K., Spudich, J. L. 1993 Comparative study of phototactic and photophobic receptor chromophore properties in *Chlamydomonas reinhardtii*. *Biophys. J.* **65**, 508–518.

[15] Kröger, P. & Hegemann, P. 1994 Photophobic responses and phototaxis in Chlamydomonas are triggered by a single rhodopsin photoreceptor. *FEBS Lett.* **341**, 5-9.

[16] Bennoun, P. 1982 Evidence for a respiratory chain in the chloroplast. *Proc. Natl. Acad. Sci. USA* **79**, 4352–4356.

[17] Jans, F., Mignolet, E., Houyoux, P. A., Cardol, P., Ghysels, B., Cuiné, S., Cournac, L., Peltier, G., Remacle, C., Franck, F. 2008 A type II NAD(P)H dehydrogenase mediates light-independent plastoquinone reduction in the chloroplast of Chlamydomonas. *Proc. Natl. Acad. Sci. USA* **105**, 20546-20551.

[18] McDonald, A. E., Ivanov, A. G., Bode, R., Maxwell, D. P., Rodermel, S. R., Hüner, N. P. 2011 Flexibility in photosynthetic electron transport: the physiological role of plastoquinol terminal oxidase (PTOX). *Biochim. Biophys. Acta.* **1807**, 954-967.

[19] Mehler, A.H. 1957 Studies on reactions of illuminated chloroplasts. I. Mechanism of the reduction of oxygen and other Hill reagents. *Arch. Biochem. Biophys.* **33**, 65–77.

[20] Horton, P., Ruban, A. V., Walters, R. G. 1996 Regulation of light harvesting in green plants. *Annu. Rev. Plant Physiol. Plant Mol. Biol.* **47**, 655-684.

[21] Niyogi, K. K. 1999 Photoprotection revisited: genetic and molecular approaches. *Annu. Rev. Plant. Physiol. Plant Mol. Biol.* **50**, 333–359.

[22] Horton, P. & Hague, A. 1988 Studies on the induction of chlorophyll fluorescence in isolated barley protoplasts: IV. Resolution of non-photochemical quenching. *Biochim. Biophys. Acta.* **932**, 107–115.

[23] Pfundel, E. E. & Dilley, R. A. 1993 The pH dependence of violaxanthin deepoxidation in isolated pea chloroplasts. *Plant Physiol.* **101**, 65–71.

[24] Gilmore, A. M. 1997 Mechanistic aspects of xanthophyll cycle-dependent photoprotection in higher plant chloroplasts and leaves. *Physiol. Plant.* **99**, 197-209.

[25] Müller, P., Li, X. P., Niyogi, K. K. 2001 Non-photochemical quenching. A response to excess light energy. *Plant Physiol.* **125**, 1558-1566.

[26] Hope, A. B. 1993 The chloroplast cytochrome b6f complex: a critical focus on function. *Biochim. Biophys. Acta.* **1143**, 1–22.

[27] Rochaix, J. D. 2011 Regulation of photosynthetic electron transport. *Biochim. Biophys. Acta.* **1807**, 375-383.

[28] Rochaix, J. D., Lemeille, S., Shapiguzov, A., Samol, I., Fucile, G., Willig, A., Goldschmidt-Clermont, M. 2012 Protein kinases and phosphatases involved in the acclimation of the photosynthetic apparatus to a changing light environment. *Philos. Trans. R. Soc. Lond. B. Biol. Sci*. **367**, 3466-3474.

[29] Aro, E.M., Kettunen, R., Tyystjärvi, E. 1992 ATP and light regulate D1 protein modification and degradation. Role of D1* in photoinhibition. *FEBS Lett.* **297**, 29-33.

[30] Bailey, S., Melis, A., Mackey, K. R., Cardol, P., Finazzi, G., van Dijken, G., Berg, G.M., Arrigo, K., Shrager, J., Grossman, A. 2008 Alternative photosynthetic electron flow to oxygen in marine Synechococcus. *Biochim. Biophys. Acta.* **1777**, 269-276.

[31] Cardol, P., Bailleul, B., Rappaport, F., Derelle, E., Béal, D., Breyton, C., Bailey, S., Wollman, F. A., Grossman, A., Moreau, H., Finazzi, G. 2008 An original adaptation of photosynthesis in the marine green alga Ostreococcus. *Proc. Natl. Acad. Sci. USA* **105**, 7881–7886.

[32] Li, X. P., Björkman, O., Shih, C., Grossman, A. R., Rosenquist, M., Jansson, S., Niyogi, K. K. 2000 A pigment-binding protein essential for regulation of photosynthetic light harvesting. *Nature* **403**, 391-395.

[33] Bonente, G., Passarini, F., Cazzaniga, S., Mancone, C., Buia, M. C., Tripodi, M., Bassi, R., Caffarri, S. 2008 The occurrence of the psbS gene product in *Chlamydomonas reinhardtii* and in other photosynthetic organisms and its correlation with energy quenching. *Photochem. Photobiol.* **84**, 1359-1370.

[34] Koziol, A. G., Borza, T., Ishida, K., Keeling, P., Lee, R. W., Durnford, D. G. 2007 Tracing the evolution of the light-harvesting antennae in chlorophyll a/b-containing organisms. *Plant Physiol.* **143**, 1802-1816.

[35] Peers, G., Truong, T. B., Ostendorf, E., Busch, A., Elrad, D., Grossman, A.R., Hippler, M., Niyogi, K. K. 2009 An ancient light-harvesting protein is critical for the regulation of algal photosynthesis. *Nature* **462**, 518-521.

[36] Delosme, R., Olive, J., Wollman, F. A. 1996 Changes in light energy distribution upon state transitions: an in vivo photoacoustic study of the wildtype and photosynthesis mutants from *Chlamydomonas reinhardtii*. *Biochim. Biophys. Acta* **1273**, 150–158.

[37] Rintamaki, E., Martinsuo, P., Pursiheimo, S., Aro, E. M. 2000 Cooperative regulation of light-harvesting complex II phosphorylation via the plastoquinol and ferredoxin-thioredoxin system in chloroplasts. *Proc. Natl. Acad. Sci. USA* **97**, 11644–11649.

[38] Martinsuo, P., Pursiheimo, S., Aro, E. M., Rintamaki, E. 2003 Dithiol oxidant and disulfide reductant dynamically regulate the phosphorylation of lightharvesting complex II proteins in thylakoid membranes. *Plant Physiol.* **133**, 37–46.

[39] Lemeille, S., Willig, A., Depège-Fargeix, N., Delessert, C., Bassi, R., Rochaix, J. D. 2009 Analysis of the chloroplast protein kinase Stt7 during state transitions. *PLoS Biol.* **7**, e45.

[40] Allen, J. F., Bennett, J., Steinback, K. E., Arntzen, C.J. 1981 Chloroplast protein phosphorylation couples plastoquinone redox state to distribution of excitation energy between photosystems. *Nature* **291**, 25 – 29.

[41] Vener, A. V., Van Kan, P. J., Gal, A., Andersson, B., Ohad, I. 1995 Activation/deactivation cycle of redoxcontrolled thylakoid protein phosphorylation. Role of plastoquinol bound to the reduced cytochrome bf complex. *J. Biol. Chem.* **270**, 25225–25232.

[42] Zito, F., Finazzi, G., Delosme, R., Nitschke, W., Picot, D., Wollman, F. A. 1999 The Qo site of cytochrome b6f complexes controls the activation of the LHCII kinase. *EMBO J.* **18**, 2961–2969.

[43] Shapiguzov, A., Ingelsson, B., Samol, I., Andres, C., Kessler, F., Rochaix, J. D., Vener, A. V., Goldschmidt-Clermont, M. 2010 The PPH1 phosphatase is specifically involved in LHCII dephosphorylation and state transitions in Arabidopsis. *Proc. Natl Acad. Sci. USA* **107**, 4782–4787.

[44] Pribil, M., Pesaresi, P., Hertle, A., Barbato, R., Leister, D. 2010 Role of plastid protein phosphatase TAP38 in LHCII dephosphorylation and thylakoid electron flow. *PLoS Biol.* **8**, e1000288.

[45] Avenson, T. J., Cruz, J. A., Kanazawa, A., Kramer, D. M. 2000 Regulating the proton budget of higher plant photosynthesis. *Proc. Natl. Acad. Sci. USA* **102**, 9709–9713.

[46] Foyer, C. H., Neukermans, J., Queval, G., Noctor, G., Harbinson, J. 2012 Photosynthetic control of electron transport and the regulation of gene expression. *J. Exp. Bot.* **63**, 1637-1661.

[47] DalCorso, G., Pesaresi, P., Masiero, S., Aseeva, E., Schünemann, D., Finazzi, G., Joliot, P., Barbato, R., Leister, D. 2008 A complex containing PGRL1 and PGR5 is involved in the switch between linear and cyclic electron flow in Arabidopsis. *Cell* **132**, 273-285.

[48] Takahashi, S., Milward, S. E., Fan, D. Y., Chow, W.S., Badger, M. R. 2009 How does cyclic electron flow alleviate photoinhibition in Arabidopsis? *Plant Physiol.* **149**, 1560-1567.

[49] Allorent, G., Tokutsu, R., Roach, T., Peers, G., Cardol, P., Girard-Bascou, J., Seigneurin-Berny, D., Petroutsos, D., Kuntz, M., Breyton, C., Franck, F., Wollman, F. A., Niyogi, K. K., Krieger-Liszkay, A., Minagawa, J., Finazzi, G. 2013 A dual strategy to cope with high light in *Chlamydomonas reinhardtii*. *Plant Cell* **25**, 545-557.

[50] Finazzi, G., Furia, A., Barbagallo, R. P., Forti, G. 1999 State transitions, cyclic and linear electron transport and photophosphorylation in *Chlamydomonas reinhardtii*. *Biochim. Biophys. Acta.* **1413**, 117–129.

[51] Finazzi, G., Rappaport, F., Furia, A., Fleischmann, M., Rochaix, J. D., Zito, F., Forti, G. 2002 Involvement of state transitions in the switch between linear and cyclic electron flow in *Chlamydomonas reinhardtii*. *EMBO. Rep.* **3**, 280–285.

[52] Iwai, M., Takizawa, K., Tokutsu, R., Okamuro, A., Takahashi, Y., Minagawa, J. 2010 Isolation of the elusive supercomplex that drives cyclic electron flow in photosynthesis. *Nature* **464**, 1210–1213.

[53] Minagawa, J. 2011 State transitions--the molecular remodeling of photosynthetic supercomplexes that controls energy flow in the chloroplast. *Biochim. Biophys. Acta.* **1807**, 897–905.

[54] Takahashi, H., Clowez, S., Wollman, F. A., Vallon, O., Rappaport, F. 2013 Cyclic electron flow is redox-controlled but independent of state transition. *Nat. Commun.* **4**, 1954.

[55] Locke, J. C., Kozma-Bognár, L., Gould, P. D., Fehér, B., Kevei, E., Nagy, F., Turner, M. S., Hall, A., Millar, A. J. 2006 Experimental validation of a predicted feedback loop in the multi-oscillator clock of *Arabidopsis thaliana*. *Mol. Syst. Biol.* **2**, 59.

[56] Laisk, A., Eichelmann, H. & Oja, V. 2006 C3 photosynthesis *in silico*. *Photosynth. Res.* **90**, 45-66.

[57] Samaga, R. & Klamt, S. 2013 Modeling approaches for qualitative and semi-quantitative analysis of cellular signaling networks. *Cell. Commun. Signal.* **11**, 43.

[58] Ebenhöh, O., Houwaart, T., Lokstein, H., Schlede, S., Tirok, K. 2011 A minimal mathematical model of nonphotochemical quenching of chlorophyll fluorescence. *Biosystems* **103**, 196-204.

[59] Zaks, J., Amarnath, K., Kramer, D.M., Niyogi, K.K., Fleming, G.R. 2012 A kinetic model of rapidly reversible nonphotochemical quenching. *Proc Natl Acad Sci USA* **109**, 15757-15762.

[60] Rochaix, J.D., Lemeille, S., Shapiguzov, A., Samol, I., Fucile, G., Willig, A., Goldschmidt-Clermont, M. 2012 Protein kinases and phosphatases involved in the acclimation of the photosynthetic apparatus to a changing light environment. *Philos Trans R Soc Lond B Biol Sci* **367,** 3466-3474.

[61] Bulte, L., Gans, P., Rebeille, F., Wollman, F.A. 1990 ATP control on state transitions *in vivo* in *Chlamydomonas reinhardtii*. *Biochim. Biophys. Acta.* **1020**, 72-80.

[62] Bonaventura, C. & Myers, J. 1969 Fluorescence and oxygen evolution from *Chlorella pyrenoidosa*. *Biochim Biophys Acta* **189,** 366-383.

[63] Rintamaki, E., Salonen, M., Suoranta, U.M., Carlberg, I., Andersson, B., Aro, E.M. 1997 Phosphorylation of light-harvesting complex II and photosystem II core proteins shows different irradiance-dependent regulation in vivo. Application of phosphothreonine antibodies to analysis of thylakoid phosphoproteins. *J Biol Chem* **272**, 30476-30482.

[64] Lemeille, S. & Rochaix, J.D. 2010 State transitions at the crossroad of thylakoid signalling pathways. *Photosynth Res* **106:** 33-46

[65] Vink, M., Zer, H., Alumot, N., Gaathon, A., Niyogi, K., Herrmann, R.G., Andersson, B., Ohad, I. 2004 Light-modulated exposure of the light-harvesting complex II (LHCII) to protein kinase(s) and state transition in *Chlamydomonas reinhardtii* xanthophyll mutants. *Biochemistry* **43**, 7824-783.

[66] Owens, T.G. 1986 Light-harvesting function in the diatom *Phaeodactylum tricornutum*. II. Distribution of excitation energy between the photosystems. *Plant Physiol* **80**, 739–746.

[67] Lavaud, J., Rousseau, B., van Gorkom, H.J., Etienne, A.L. (2002) Influence of the diadinoxanthin pool size on photoprotection in the marine planktonic diatom *Phaeodactylum tricornutum*. *Plant Physiol* **129**, 1398-1406

Figure 1A

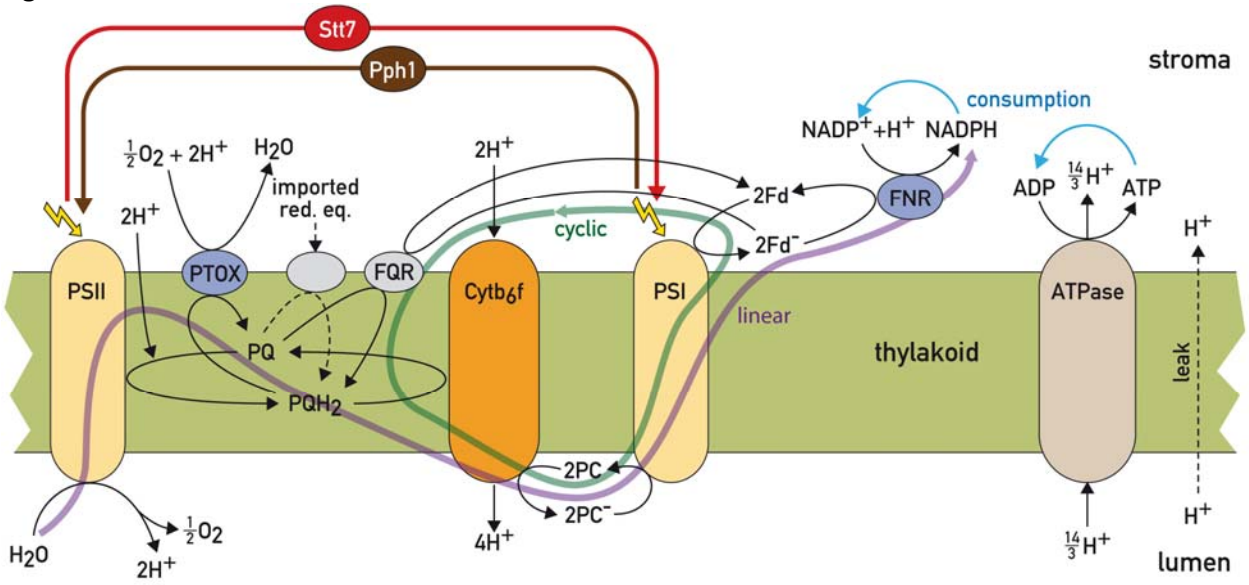

Figure 1B

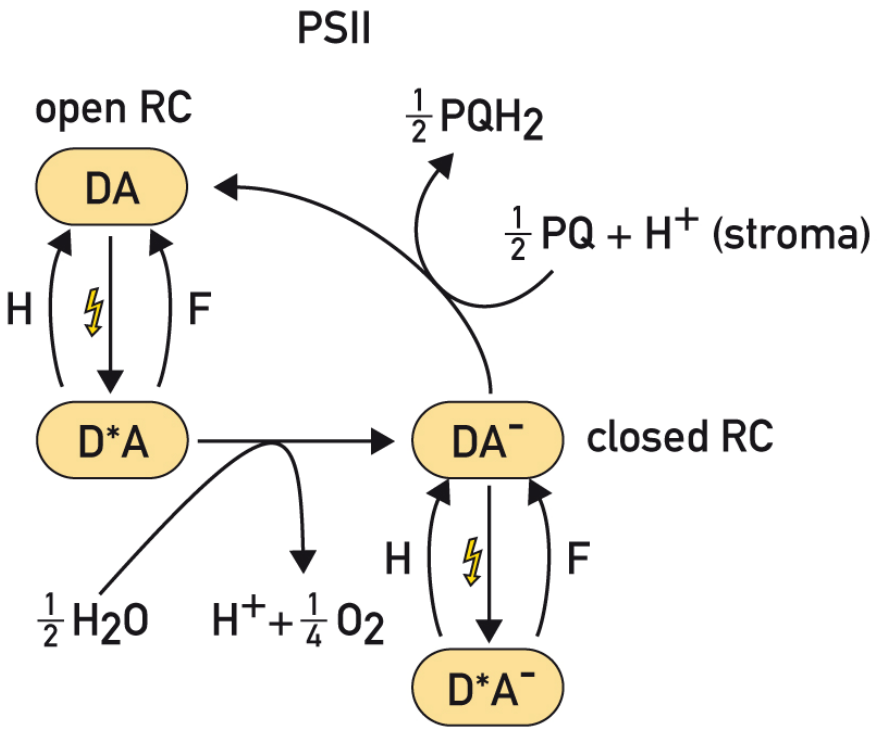

Figure 1- A) Schematic representation of the model of the photosynthetic electron transport chain and state transitions. All processes included in the mathematical model are depicted. The model includes linear and cyclic electron flow, ATP generation and a dynamic adjustment of antenna cross-sections. Linear electron flow (purple arrow) comprises photosystem II (PSII), the cytochrome b6f complex (Cytb_6f), photosystem I (PSI) and the ferredoxin-NADPH reductase (FNR). PSII is treated as a light-activated oxidoreductase transferring electrons from water to plastoquinone (PQ), resulting in the

reduced form PQH_2. In this process, two protons are taken up from the stromal side of the thylakoid membrane and two protons, resulting from splitting water, are released to the lumen. Cytb_6f is modelled as an oxidoreductase transferring electrons from PQH_2 to plastocyanin (PC), which simultaneously uses a process called the Q-cycle to release four protons in the lumen. PSI is treated as the second light-activated oxidoreductase, transferring electrons from reduced PC (PC^-) to Ferredoxin (Fd). The final step in the linear electron transport chain is catalysed by FNR, which transfers electrons from reduced Fd (Fd^-) to $NADP^+$ resulting in the formation of NADPH. Cyclic electron flow (green arrow) is represented by a single pathway involving ferredoxin-plastoquinone reductase (FQR), which transfers electrons from Fd^- back to PQ. Additionally, the model includes processes of the chlororespiratory pathway. Under aerobic conditions, the plastoquinone terminal oxidase (PTOX) oxidises the PQ pool. In anaerobic conditions, electrons, e.g. from glycolysis, are imported into the chloroplast and lead to a reduction of the PQ pool by NADH dehydrogenase (NDH). Linear and cyclic electron flow lead to a net translocation of protons into the lumen. The resulting proton gradient drives the ATP synthase (ATPase). The net products of photosynthetic electron transport, ATP and NADPH, are consumed by external processes that are simulated as lumped reactions. State transitions are modelled by two processes, relocation of antenna complexes from PSII to PSI and vice versa. The former is triggered by the kinase Stt7, while the latter is dependent on the phosphatase Pph1. In the model, Stt7 is activated by a reduced PQ pool while Pph1 is constitutively active. For details on the kinetics, see the Supplementary Text.

B) Schematic representation of the internal processes modelled in PSII. This simplified description of PSII is implemented to calculate the reaction rate of PSII and the fluorescence emitted from PSII (see Supplementary Text for details). Open reaction centres (DA) are excited by light (yellow flash). The excited state (D^*A) can either relax to the ground state DA by heat emission (H) or fluorescence (F), or it can perform charge separation and recharge the donor side through water splitting, resulting in the closed state (DA^-). The closed state is also excited by light, resulting in state D^*A^-, which can only relax back to the unexcited state DA^- either by heat (H) or fluorescence (F) emission. Closed reaction centres are re-opened by electron transfer to the PQ pool.

Figure 2

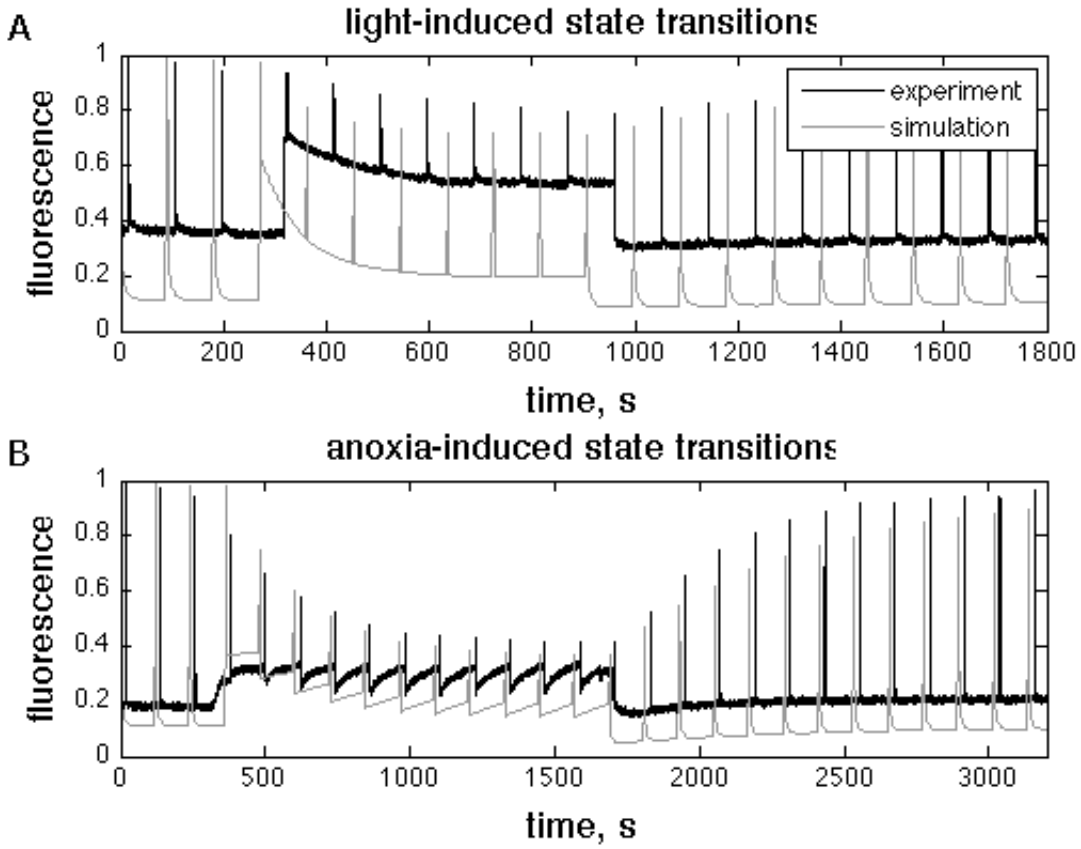

Figure 2 – Experimental (black) and simulated (grey) fluorescence traces. A Dark-adapted Chlamydomonas cells were further incubated in the dark for 5 minutes, exposed for 10 minutes to weak light (100 µE $m^{-2}s^{-1}$), and then returned to darkness. Saturating light flashes were applied at regular intervals and the fluorescence signal (black) was recorded. The same protocol was simulated with the mathematical model and the calculated fluorescence signal (grey) is shown. The dynamics of F_M reflect the transition to state 2 in the light and the reverse transition to state 1 in darkness. B Anoxia was induced by sealing the culture and allowing respiration to consume the available oxygen. After 15 minutes of anoxia air was re-applied by bubbling in the sample. Saturating flashes were applied at regular intervals. The experimental (black) and simulated (grey) fluorescence are shown. Again, the F_M dynamics represent transitions to state 2 in anoxic and to state 1 in aerobic conditions. The F_s dynamics between flashes reflect the redox poise of the PQ pool.

Figure 3

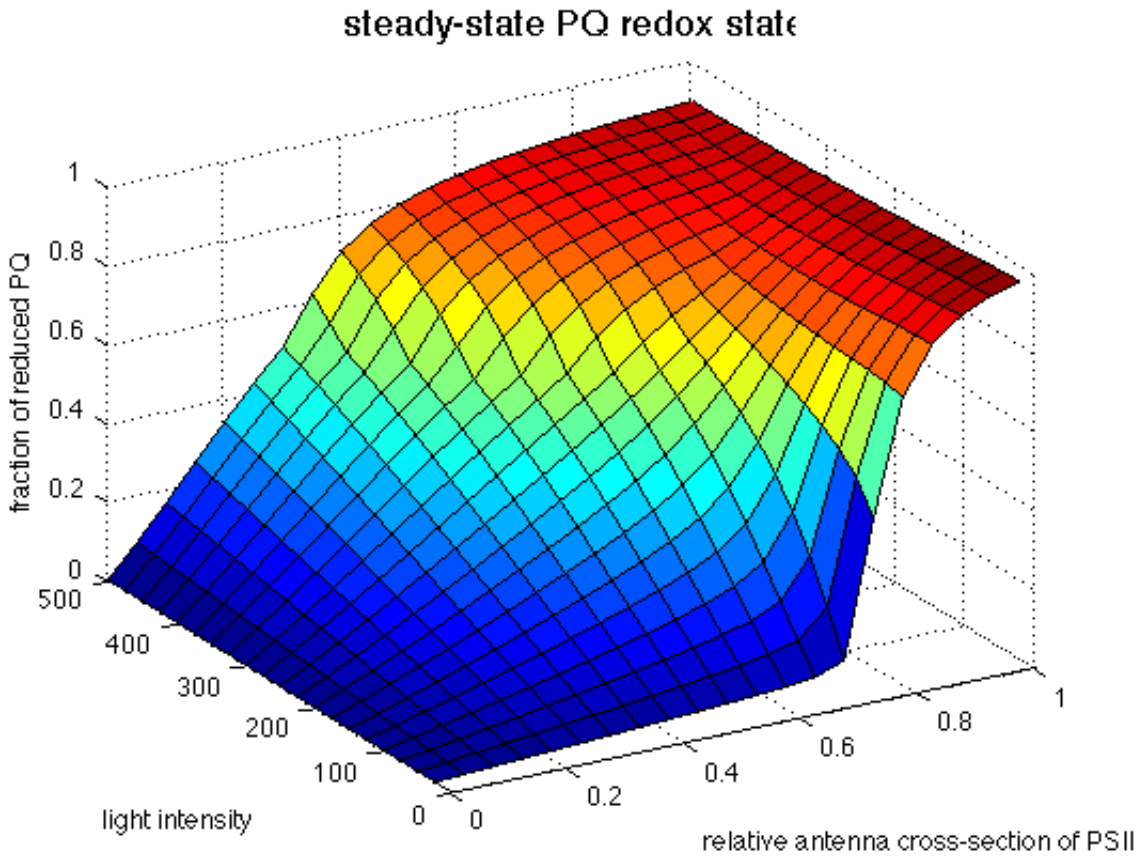

Figure 3 – Predicted stationary states of the reduction level of the PQ pool for different light intensities and different states. For these predictions, state transition were modelled by imposing values for the relative antenna cross-sections (x-axis) between 0, representing all antennae on PSI, and 1, representing all antennae on PSII and keeping them fixed throughout the simulations. Light intensity (y-axis) was varied and for each combination of light intensity and antenna cross-sections, the system was simulated until steady state was reached. On the z-axis the reduced fraction of the PQ pool in stationary state is plotted. For low light intensities, a sharp transition between a strongly oxidised and a highly reduced PQ pool is observed, demonstrating that only tightly controlled cross-sections can ensure a balanced redox poise and thus explaining the importance of state transitions in this low light regime. For higher light intensities the transition is smoother, indicating a higher flexibility in cross-section to achieve redox poise.

Supplementary Figure S1

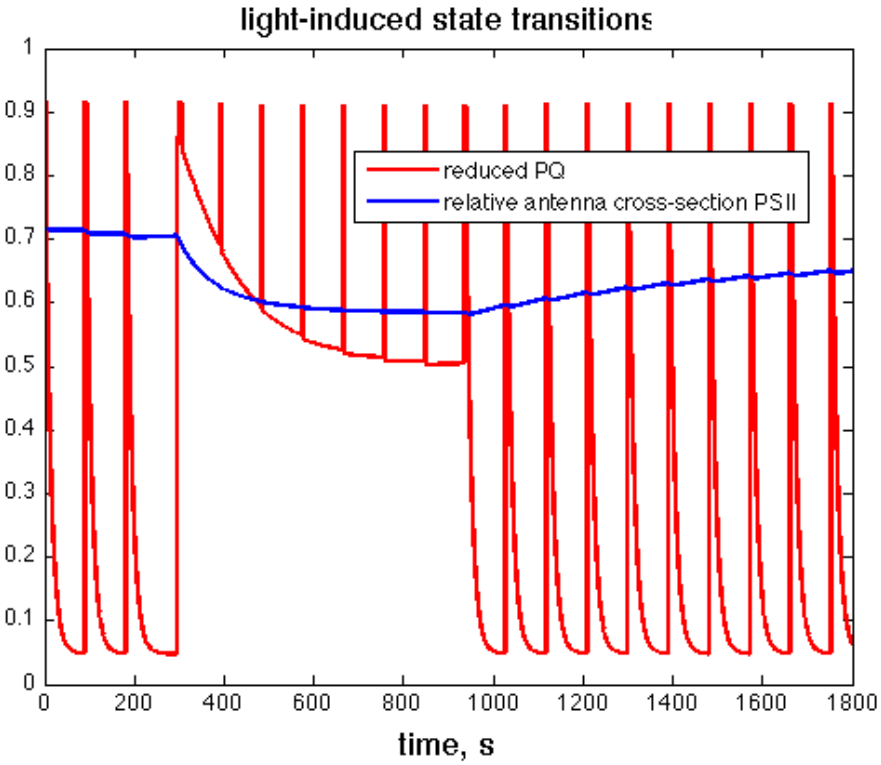

Simulated temporal evolution of the plastoquinone redox state (red) and the antenna cross-section of PSII (blue) as a response to light-induced state transitions. The same simulation protocol as for Fig. 2A in the main text was used. In the dark periods, the saturating flashes lead to a transient reduction of PQ, which is re-oxidised within several seconds. During constant illumination, the PQ pool is reduced, triggering state transitions. As a result, antenna cross-section associated with PSII is reduced. In the model simulation, only 10% of all antenna are relocated from PSII to PSI, reducing the relative cross-section of PSII from 0.7 to 0.6. This relocation is sufficient to establish redox poise, which is achieved near the end of the illumination period when approximately 45% of PQ oxidised. This process is slowly reversed in the dark.

Supplementary Figure S2

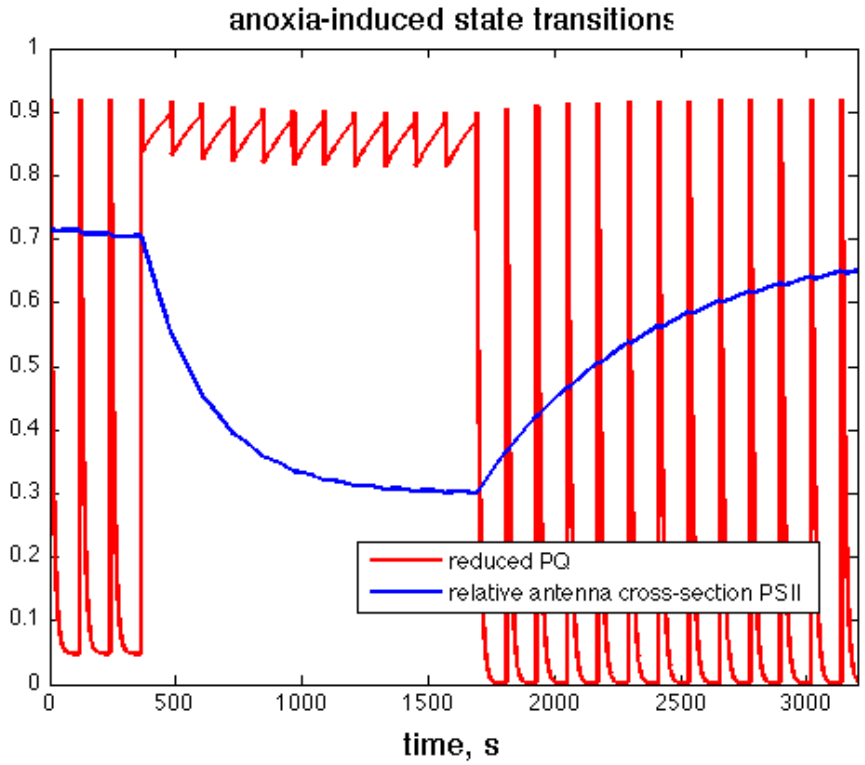

Simulated temporal evolution of the plastoquinone redox state (red) and the antenna cross-section of PSII (blue) as a response to anoxia-induced state transitions. The same simulation protocol as for Fig. 2B in the main text was used. Under aerobic conditions, saturating flshes lead to a transient reduction of PQ, which is re-oxidised within several seconds. During anoxia, PQ is permanently reduced, thus inducing state transitions. In contrast to the light-induced case, reducing the cross-section of PSII does not lead to a less reduced PQ, thus the regulatory feedback is not operating. This results in a more complete state transition in which approximately 40% of the antenna are relocated from PSII to PSI.

Supplementary Figure S3

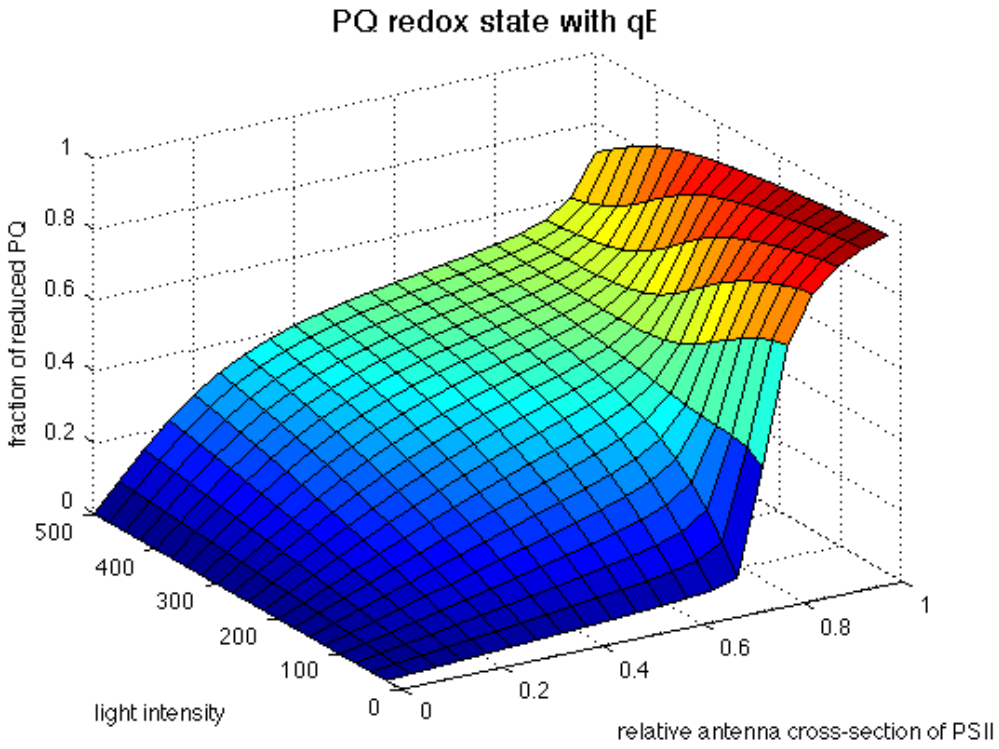

Same as Figure 3 in the main text, but with a qE-dependent quenching mechanism included in the model. For varying light intensity (x-axis) and varying relative antenna cross-sections (y-axis), the stationary fraction of the oxidised fraction of the PQ pool is plotted (z-axis). Comparison to Figure 3 of the main text shows little difference for low light intensity, where a sharp transition between oxidised and reduced PQ can be observed. However, for high light intensities, qE-dependent quenching leads to the establishment of a plateau, where for a wide range of antenna cross-sections the redox state of the PQ pool remains approximately constant. This demonstrates how qE-dependent quenching establishes a redox poise and explains why state transitions, at least in the presence of qE quenching, do not play an important role under high light.

A mathematical model of the photosynthetic electron transport chain

S1 Stoichiometry of the model

The mathematical model of the electron transport chain including dynamics of the state transitions is represented as a system of seven ordinary differential equations governing the temporal evolution of seven variables. These variables are 1) the oxidised fraction of the plastoquinone pool (P), 2) the oxidised fraction of the plastocyanin pool (C), 3) the oxidised fraction of the ferredoxin pool (F), 4) the stromal concentration of ATP (T), 5) the stromal concentration of NADPH (N), 6) the lumenal proton concentration (H) and 7) the fraction of mobile antenna which are associated with photosystem II (A).

The system of equations reads

$$\begin{aligned}
\frac{dP}{dt} &= -v_{\mathrm{PSII}} + v_{\mathrm{b6f}} - v_{\mathrm{FQR}} + v_{\mathrm{PTOX}} - v_{\mathrm{NDH}} && (1)\\
\frac{dC}{dt} &= -2v_{\mathrm{b6f}} + v_{\mathrm{PSI}} && (2)\\
\frac{dF}{dt} &= -v_{\mathrm{PSI}} + 2v_{\mathrm{FNR}} + 2v_{\mathrm{FQR}} && (3)\\
\frac{dT}{dt} &= v_{\mathrm{ATPsynthase}} - v_{\mathrm{ATPconsumption}} && (4)\\
\frac{dN}{dt} &= v_{\mathrm{FNR}} - v_{\mathrm{NADPHconsumption}} && (5)\\
b_H \cdot \frac{dH}{dt} &= 2v_{\mathrm{PSII}} + 4v_{\mathrm{b6f}} - \frac{14}{3}v_{\mathrm{ATPsynthase}} - v_{\mathrm{leak}} && (6)\\
\frac{dA}{dt} &= -v_{\mathrm{Stt7}} + v_{\mathrm{Pph1}}. && (7)
\end{aligned}$$

The various rates are functions of the dynamic variables, external constants and parameters. Their functional form is described and explained below. Parameters are given in Table S1. Unless stated otherwise, the units used in the model are all given in moles per mole chlorophyll. As in [1], we assume a Chlorophyll content of $350 \cdot 10^{-6}$ mol per m^2 thylakoid membrane and lumen and stroma volumes of 0.0014 l m^{-2} and 0.0112 l m^{-2}, respectively [2]. Thus, 1 mmol(mol Chl)$^{-1}$ corresponds to $2.5 \cdot 10^{-4}$M in the lumen and $3.2 \cdot 10^{-5}$M in the stroma. Also as in [2], we assume a constant buffering of protons in the lumen, represented by the constant b_H.

S2 Rate equations

Most rate equations are formulated based on the maximum parsinomy principle. If no other evidence is given, we employ the simplest functional form that appears reasonable. The rationale behind this approach is to determine the simplest set of equations which realistically describes the system. Most rate equations therefore are described by simple mass-action or Michaelis-Menten kinetcs. Exceptions are those for the two photosystems v_{PSI} and v_{PSII}, which are described in more detail in a separate section below.

Cytochrome $\mathbf{b_6f}$ The chemical formula for the net reaction of cytochrome b_6f is

$$\mathrm{PQH_2} + 2\,\mathrm{PC} + 2\,\mathrm{H^+_{stroma}} \rightleftharpoons \mathrm{PQ} + 2\,\mathrm{PC^-} + 4\,\mathrm{H^+_{lumen}}. \tag{8}$$

The equilibrium of this reaction is therefore dependent on the stromal and lumenal proton concentration. How equilibrium constants are determined as functions of the pH is described below. We approximate the rate of the b_6f complex by a simple mass-action kinetics:

$$v_{\mathrm{b6f}} = \max\left(k_{\mathrm{b6f}} \cdot \left((\mathrm{PQ^{tot}} - P)\cdot C^2 - \frac{P\cdot(\mathrm{PC^{tot}} - C)^2}{K_{\mathrm{eq,b6f}}(H)}\right), v^{\mathrm{min}}_{\mathrm{b6f}}\right). \tag{9}$$

Here, $\mathrm{PQ^{tot}}$ and $\mathrm{PC^{tot}}$ are constants reflecting the (conserved) total plastoquinone and plastocyanin pools, respectively. Thus, $\mathrm{PQ^{tot}} - P$ denotes the reduced fraction of the plastoquinone pool and likewise for plastocyanin. The minimal rate $v^{\mathrm{min}}_{\mathrm{b6f}}$ has been introduced to avoid an extremely rapid export of protons if the lumenal pH drops below a value at which the direction of the reaction of cytochrome b_6f is reverted.

FNR The reaction mediated by FNR is

$$2\,\mathrm{Fd^-} + \mathrm{NADP^+} + \mathrm{H^+_{stroma}} \rightleftharpoons 2\,\mathrm{Fd} + \mathrm{NADPH}. \tag{10}$$

Since for this enzyme K_{M}-values have been determined, we use a more realistic rate equation by employing the convenience kinetics developed in [3], resulting in

$$v_{\mathrm{FNR}} = V^{\mathrm{max}}_{\mathrm{FNR}} \cdot \frac{f^{-2}\cdot n^+ - (f^2\cdot n)/K_{\mathrm{eq,FNR}}}{(1+f^-+f^{-2})\cdot(1+n^+) + (1+f+f^2)\cdot(1+n^+) - 1}, \tag{11}$$

where f, f^-, n^+ and n are the normalised concentrations

$$f = \frac{F}{K_{\mathrm{M,F}}},\ f^- = \frac{\mathrm{Fd^{tot}} - F}{K_{\mathrm{M,F}}},\ n^+ = \frac{\mathrm{NADP^{tot}} - N}{K_{\mathrm{M,N}}},\ n = \frac{N}{K_{\mathrm{M,N}}}, \tag{12}$$

where $\mathrm{Fd^{tot}}$ and $\mathrm{NADP^{tot}}$ are constants reflecting the total pools of ferredoxin and nicotinamide nucleotide phosphates, respectively and $K_{\mathrm{eq,FNR}}$ is the equilibrium constant determined by standard potentials as described below.

Cyclic electron flow We assume that electrons from ferredoxin can be re-injected into the plastoquinone pool by the ferredoxin-plastoquninone reductase FQR, resulting in a cyclic electron flow, according to the chemical equation

$$2\,\mathrm{Fd}^- + \mathrm{PQ} + 2\,\mathrm{H}^+_{\mathrm{stroma}} \rightarrow 2\mathrm{Fd} + \mathrm{PQH}_2. \tag{13}$$

For this, we employ a simple mass-action kinetic rate law.

$$v_{\mathrm{FQR}} = k_{\mathrm{FQR}} \cdot (\mathrm{Fd}^{\mathrm{tot}} - F)^2 \cdot P. \tag{14}$$

This reaction is practically irreversible. In principle, electrons can also be re-injected into the PQ pool from NADPH. Both mechanisms lead to the same overall effect. For simplicity and due to the fact that the molecular details as well as the kinetic properties of the proteins mediating the cyclic flow are not yet fully understood, we decided to include only one cyclic flow, by assuming that FQR catalyses the reduction of plastoquinone by the oxidation of ferredoxin. With the information currently available, including one or two mechanisms to re-inject electrons into the PQ pool does not result in significant differences.

ATP synthase ATP synthesis is modelled as in [1] with a mass-action kinetics and a lumenal pH-dependent equilibrium constant.

$$v_{\mathrm{ATPsynthase}} = k_{\mathrm{ATPsynthase}} \cdot \left(\mathrm{AP}^{\mathrm{tot}} - T - \frac{T}{K_{\mathrm{eq,ATPsynthase}}(H)} \right), \tag{15}$$

where $\mathrm{AP}^{\mathrm{tot}}$ is the constant total adenosine phosphate pool.

Proton leak A small leak current of protons over the thylakoid membrane is introduced and modelled with mass-action kinetics.

$$v_{\mathrm{leak}} = k_{\mathrm{leak}} \cdot (H - \mathrm{H}^+_{\mathrm{stroma}}). \tag{16}$$

Consuming reactions For simplicity, we model ATP and NADPH consuming processes as simple mass-action kinetics. This is certainly an over-simplification and does not reflect the coupled demand through the Calvin-Benson cycle, the main consuming process. However, it already allows to assess how changes in the ratio affect the electron transport chain. We employ the following equations for the consumption processes

$$v_{\mathrm{ATPconsumption}} = k_{\mathrm{ATPconsumption}} \cdot T, \tag{17}$$

$$v_{\mathrm{NADPHconsumption}} = k_{\mathrm{NADPHconsumption}} \cdot N. \tag{18}$$

Oxidation and reduction of the PQ pool In the presence of oxygen, the plastoquinone terminal oxidase catalyses the oxidation of the plastoquinone pool. This is modelled as a simple mass-action rate law.

$$v_{\mathrm{PTOX}} = k_{\mathrm{PTOX}} \cdot \mathrm{O}_2^{\mathrm{ext}} \cdot (\mathrm{PQ}^{\mathrm{tot}} - P). \tag{19}$$

In the absence of oxygen, electrons from external sources, such as glycolysis, lead to a slow reduction of the plastoquinone pool, which can be mediated by the NADH reductase NDH. We assume a simple mass-action rate law according to

$$v_{\mathrm{NDH}} = k_{\mathrm{NDH}} \cdot P. \tag{20}$$

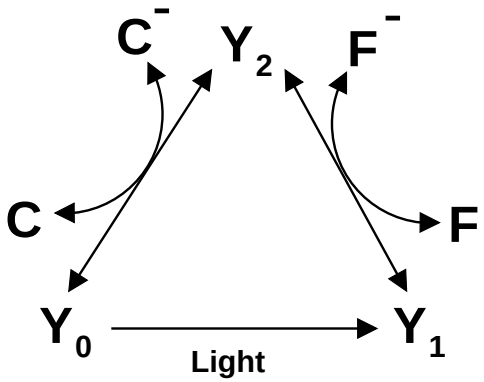

Figure S4: Schematic representation of Photosystem I. Y_0 (P_{700}) is activated by light to Y_1 ($P^{\star}_{700}$), which reduces ferredoxin (F) with its concomitant oxidation to Y_2 (P^{+}_{700}). Y_2 is reduced by plastocyanin (C^{-}) to Y_0.

S3 Photosystems

Activation by light The light intensity (photon flux density – PFD) is given in μmol photons m^{-2} s^{-1}. A conversion factor c_{PFD} which is fitted is applied to convert the photon flux density into activation rates. The activation rates for the two photosystems are multiplied by the relative cross-sections σ_{I} and σ_{II}. These are calculated from the fractions of antenna fixed to PSI and PSII (σ^0_{I} and σ^0_{II}, respectively) and the variable A representing the fraction of mobile antenna associated with PSII by

$$\sigma_{\mathrm{I}} = \sigma^0_{\mathrm{I}} + (1-A)\cdot(1-\sigma^0_{\mathrm{I}}-\sigma^0_{\mathrm{II}}), \tag{21}$$

$$\sigma_{\mathrm{II}} = \sigma^0_{\mathrm{II}} + A\cdot(1-\sigma^0_{\mathrm{I}}-\sigma^0_{\mathrm{II}}). \tag{22}$$

With this, the activation rates for PSI and PSII are

$$k_{\mathrm{LI}} = c_{\mathrm{PFD}}\cdot\sigma_{\mathrm{I}}\cdot\mathrm{PFD}, \tag{23}$$

$$k_{\mathrm{LII}} = c_{\mathrm{PFD}}\cdot\sigma_{\mathrm{II}}\cdot\mathrm{PFD}. \tag{24}$$

Photosystem I Photosystem I is described as a light-activated oxidoreductase performing the net transformation

$$\mathrm{PC}^{-} + \mathrm{Fd} \rightarrow \mathrm{PC} + \mathrm{Fd}^{-}. \tag{25}$$

The transformation can be simplified to work according to the scheme in Fig. S4 The single steps are assumed to proceed according to mass-action kinetics. To determine the overall activity, the fraction of open PSI (Y_0) is determined by a quasi steady-state approximation. For the calculation, the two differential equations

$$0 = \frac{dY_0}{dt} = k_{\mathrm{PCox}}\cdot(\mathrm{PC}^{\mathrm{tot}}-C)\cdot Y_2 - \frac{k_{\mathrm{PCox}}}{K_{\mathrm{eq,PCP700}}}\cdot C\cdot Y_0 - k_{\mathrm{LI}}Y_0 \tag{26}$$

$$0 = \frac{dY_1}{d1} = k_{\mathrm{LI}}Y_0 - k_{\mathrm{Fdred}}\cdot F\cdot Y_1 + \frac{k_{\mathrm{Fdred}}}{K_{\mathrm{eq,P700Fd}}}\cdot(\mathrm{Fd}^{\mathrm{tot}}-F)\cdot Y_2. \tag{27}$$

are set to zero and Y_0 is determined from the two resulting algebraic equations under consideration of the conserved quantity

$$\mathrm{PSI}^{\mathrm{tot}} = Y_0 + Y_1 + Y_2, \tag{28}$$

resulting in

$$Y_0 = \frac{\mathrm{PSI}^{\mathrm{tot}}}{1 + \frac{k_{\mathrm{LI}}}{k_{\mathrm{Fdred}} \cdot F} + \left(1 + \frac{F}{K_{\mathrm{eq,P700Fd}}(\mathrm{Fd}^{\mathrm{tot}} - F)}\right) \cdot \left(\frac{\mathrm{PC}^{\mathrm{tot}} - C}{K_{\mathrm{eq,PCP700}} C} + \frac{k_{\mathrm{LI}}}{k_{\mathrm{PCox}}(\mathrm{PC}^{\mathrm{tot}} - C)}\right)}. \tag{29}$$

Here, k_{PCox} is the rate constant for oxidation of plastocyanin at P_{700}, k_{Fdred} is the rate for reduction of ferredoxin by PSI and k_{LI} is the light activation rate of PSI, which is determined by the total light intensity and the antenna cross-section of PSI. The overall rate of the oxidoreductase activity of PSI is then

$$v_{\mathrm{PSI}} = k_{LI} \cdot Y_0. \tag{30}$$

Photosystem II For PSII, a similar approach is chosen and the simplified reaction scheme is shown in Fig. 1B in the main text. Here, it is assumed that the excited states (B_1 and B_3) can revert to the ground state by either non-radiative decay (with rate k_H) or by fluorescence (with rate k_F). State B_1 can exert photochemistry (with rate k_{Pchem}), which comprises several internal steps in PSII including recharge of the donor side at the oxygen evolving complex.

The four states B_0, B_1, B_2 and B_3 are determined by a quasi steady-state approximation. For this, the three differential equations for B_0, B_1 and B_3 are set to zero and the conservation rule for PSII is exploited, leading to the algebraic linear equation system

$$\begin{aligned}
-\left(k_{\mathrm{LII}} + \frac{k_{\mathrm{PQred}}}{K_{\mathrm{eq,QAPQ}}}(\mathrm{PQ}^{\mathrm{tot}} - P)\right) B_0 + (k_H + k_F) B_1 + k_{\mathrm{PQred}} P B_3 &= 0, && (31)\\
k_{\mathrm{LII}} B_0 - (k_H + k_F + k_{\mathrm{Pchem}}) B_1 &= 0, && (32)\\
k_{\mathrm{LII}} B_2 - (k_H + k_F) B_3 &= 0, && (33)\\
B_0 + B_1 + B_2 + B_3 &= \mathrm{PSII}^{\mathrm{tot}}, && (34)
\end{aligned}$$

which is solved numerically by matrix inversion in every integration step. The overall rate of the oxidoreductase activity of PSII is then

$$v_{\mathrm{PSII}} = k_{\mathrm{LII}} \cdot B_1. \tag{35}$$

Fluorescence The status of PSII allows the calculation of the fluorescence signal. In a fluorescence monitoring system, the measuring beam is considered as non-actinic. Similar to [4], we calculate the fluorescence as the probability that an excited state is reverting to a ground state by fluorescence [5]. Thus, the fluorescence signal resulting from state B_1 is proportional to $k_F/(k_H + k_F + k_{\mathrm{Pchem}})$ and that resulting from B_3 is proportional to $k_F/(k_H + k_F)$. Further, the fluorescence signals are proportional to the occupation of the two respective ground states and both are proportional to the cross-section of PSII. These assumptions result in the following formula for the fluorescence

$$\Phi = \sigma_{\mathrm{II}} \left(\frac{k_F}{k_H + k_F + k_{\mathrm{Pchem}}} B_0 + \frac{k_F}{k_H + k_F} B_2\right). \tag{36}$$

Base fluorescence F_0 is observed when all reaction centres are open (dark, PSII predominantly in state B_0). In the model, this corresponds to a fluorescence value of $\Phi = k_F/(k_H + k_F + k_{\mathrm{Pchem}})$. Maximal fluorescence F_{M} is observed under saturating flashes,

which close all reaction centres (PSII predominantly in state B_2). This corresponds to $\Phi = k_F/(k_H + k_F)$.

The calculated fluorescence signal is not normalised. For comparison with experiments, it is normalised to the highest peak determined by simulating a saturating flash in the dark-adapted state.

S4 State transitions

For the model, we make the simplifying assumption that the kinase Stt7 is directly responsible for the relocation of antenna from PSII to PSI, while the phosphatase Pph1 is performing the reverse translocation from PSI to PSII. We further assume that antenna are always either associated with PSI or PSII. As discussed in the main text, this assumption may be incorrect and possibly lead to the underestimation of the steady-state fluorescence signal. We assume that the redox state of PQ regulates the kinase such that a reduced plastoquinone pool activates kinase activity. Thus, reduced PQ leads to a translocation of antenna to PSI. We model the activity of the kinase Stt7 by a Hill kinetics with moderate cooperativity ($n = 2$). The phosphatase is considered to be constitutively active.

$$v_{\mathrm{Stt7}} = k_{\mathrm{Stt7}} \cdot \left(1 - \frac{\left(\frac{P/\mathrm{PQ}^{\mathrm{tot}}}{K_{\mathrm{M,ST}}}\right)^{n_{\mathrm{ST}}}}{1 + \left(\frac{P/\mathrm{PQ}^{\mathrm{tot}}}{K_{\mathrm{M,ST}}}\right)^{n_{\mathrm{ST}}}} \right) \cdot A \tag{37}$$

$$v_{\mathrm{Pph1}} = k_{\mathrm{Pph1}} \cdot (1 - A). \tag{38}$$

Together, these kinetic rate laws lead to a plausible behaviour in that the antenna cross-section reaches a stationary state which is dependent on the redox state of the PQ pool. Reduced PQ pushes antenna towards PSI while oxidised PQ pushes antenna towards PSII. In this way, a regulatory feedback on the PQ redox state is achieved.

S5 Equilibrium constants

The equilibrium constants for the various redox reactions are calculated from midpoint potentials. For those processes involving a translocation of protons across the thylakoid membrane or the release of protons into the lumen, the resulting equilibrium constant depends on the lumenal pH. In general, the standard Gibbs free energy change ΔG^0 of a redox reaction

$$\mathrm{Ox} + \mathrm{ne}^- + \mathrm{mH}^+ \rightleftharpoons \mathrm{Red} \tag{39}$$

is

$$\Delta G^0 = -nFE^0 + mRT \ln(10) \cdot \mathrm{pH} + nFE, \tag{40}$$

where pH refers to the pH in the compartment of the free protons, E^0 is the standard redox potential of the redox couple (at pH 0), E is the redox potential of the medium, F is the Faraday constant, R the universal gas constant and T the temperature [30]. Since an overall reaction does not involve free electrons, the terms nFE will cancel in the following calculation for the overall equilibrium constant.

Table S1: Rate Parameters used throughout the paper as a reference.

parameter	value	reference/comment
Pool sizes		
PQ^{tot}	17.5 mmol(mol Chl)$^{-1}$	[6]
PC^{tot}	4 mmol(mol Chl)$^{-1}$	[7]
AP^{tot}	60 mmol(mol Chl)$^{-1}$	2mM, [8]
$NADP^{tot}$	25 mmol(mol Chl)$^{-1}$	0.8mM, [8]
Fd^{tot}	5 mmol(mol Chl)$^{-1}$	[7]
PSI^{tot}	2.5 mmol(mol Chl)$^{-1}$	[9]
$PSII^{tot}$	2.5 mmol(mol Chl)$^{-1}$	[9]
Rate constants		
k_{b6f}	2.5 mmol^{-2}(mol Chl)^2 s^{-1}	estimated from PQ→Cyt_f half-life ≈ 14ms, [10]
v_{b6f}^{min}	−2.5 mmol(mol Chl)$^{-1}$s^{-1}	ad-hoc estimate to avoid strong reverse currents
V_{FNR}^{max}	1500 mmol(mol Chl)$^{-1}$s^{-1}	[7, 11]
k_{FQR}	1 mmol^{-2}(mol Chl)^2 s^{-1}	ad-hoc value, needs to be refined as model becomes more elaborate
$k_{ATPsynthase}$	20 s^{-1}	fitted to allow a maximal production of ≈ 400 mmol(mol Chl)$^{-1}$s^{-1}, which allows for the maximal reported CO_2 fixation rate of 500 μmol reduced CO_2(μmol Chl)$^{-1}$h^{-1} [12]
$k_{ATPconsumption}$	10 s^{-1}	fitted to yield reasonable ATP:ADP under various light regimes
$k_{NADPHconsumption}$	15 s^{-1}	fitted to yield reasonable NADPH:$NADP^+$ ratios
k_{PCox}	2500 mmol^{-1}(mol Chl) s^{-1}	estimated from PC→P_{700} half-life ≈ 0.2ms, [13]
k_{Fdred}	$2.5 \cdot 10^5$ mmol^{-1}(mol Chl) s^{-1}	estimated from FB→Fd half-life ≈ 2μs, [14]
k_{PQred}	250 mmol^{-1}(mol Chl) s^{-1}	estimated from QB→PQ half-life ≈ 1ms, [15]
k_H	$5 \cdot 10^8$s^{-1}	similar to [4], where $k_H = 1/1.8\text{ns} = 5.56 \cdot 10^8\text{s}^{-1}$ was used
k_F	$6.25 \cdot 10^7$s^{-1}	[4]
k_{Pchem}	$1.2 \cdot 10^9$s^{-1}	estimated as a composite rate from various parameters from [16, 4]
k_{PTOX}	0.01mmol^{-1}(mol Chl) s^{-1}	fitted to inter-flash F_S-dynamics in aerobic conditions (Fig. 2A)
k_{NDH}	0.004 s^{-1}	fitted to inter-flash F_S-dynamics in anaerobic conditions (Fig. 2B)
k_{Stt7}	0.0035 s^{-1}	fitted to F_M-dynamics (Fig. 2A and 2B)
k_{Pph1}	0.0013 s^{-1}	fitted to F_M-dynamics (Fig. 2A and 2B)
k_{epox}	0.05 s^{-1}	[17], only needed for qE
k_{deep}	0.004 s^{-1}	[17], only needed for qE
k_H^0	$5 \cdot 10^8$ s^{-1}	[4], only needed for qE
$k_H^{dynamic}$	$5 \cdot 10^9$ s^{-1}	[4], only needed for qE
Michaelis constants		
$K_{M,F}$	1.56 mmol(mol Chl)$^{-1}$	0.05mM, [18]
$K_{M,N}$	0.22 mmol(mol Chl)$^{-1}$	0.007mM, [19, 20]
$K_{M,ST}$	0.2	estimated to yield a PQ redox poise of ≈ 1:1
$K_{M,Q}$	corresponding to pH 5.8	[17], only needed for qE
External concentrations		
H^+_{stroma}	$6.34 \cdot 10^{-5}$ mmol(mol Chl)$^{-1}$	corresponds to pH 7.8
O_2^{ext}	8 mmol(mol Chl)$^{-1}$ (0)	corresponds to 250μM or 20% in air (0 in anoxic conditions)
Other constants		
b_H	100	[2]
σ_I^0	0.2	inspired by [21, 22, 23] and fitted to F_M-dynamics (Fig. 2A and 2B)
σ_{II}^0	0	inspired by [21, 22, 23] and fitted to F_M-dynamics (Fig. 2A and 2B)
n_{ST}	2	ad-hoc value to use a reasonable cooperativity
c_{PFD}	1/3	fitted
n_Q	5	[17], only needed for qE
Standard potentials		
$E^0(QA/QA^-)$	−0.140 V	[24]
$E^0(PQ/PQH_2)$	0.354 V	[25]
$E^0(PC/PC^-)$	0.380 V	[26]
$E^0(P^+_{700}/P_{700})$	0.480 V	[27]
$E^0(FA/FA^-)$	−0.550 V	[28]
$E^0(Fd/Fd^-)$	−0.430 V	[29]
$E^0(NADP^+/NADPH)$	−0.113 V	[30]

Table S2: Redox pairs used for the calculation of equilibrium constants

reaction	e^- donor	e^- acceptor
PQ reduction at PSII	QA/QA^-	PQ/PQH_2
Cytb_6f	PQ/PQH_2	PC/PC^-
PC oxidation at PSI	PC/PC^-	P^+_{700}/P_{700}
Fd reduction at PSI	FA/FA^-	Fd/Fd^-
FNR	Fd/Fd^-	$NADP^+/NADPH$
FQR	Fd/Fd^-	PQ/PQH_2

We illustrate the calculation for the example of the overall redox reaction mediated by cytochrome b_6f. The overall reaction is (see Eq. 8)

$$PQH_2 + 2\,PC + 2\,H^+_{stroma} \rightleftharpoons PQ + 2\,PC^- + 4\,H^+_{lumen}. \tag{41}$$

We split this into two redox half-reactions and one transport process:

$$PQ + 2\,e^- + 2\,H^+_{lumen} \rightleftharpoons PQH_2 \tag{42}$$
$$PC + e^- \rightleftharpoons PC^- \tag{43}$$
$$H^+_{stroma} \rightleftharpoons H^+_{lumen}. \tag{44}$$

The overall reaction is the stoichiometric sum

$$-1 \cdot (42) + 2 \cdot (43) + 2 \cdot (44). \tag{45}$$

The three contributions to the standard Gibbs free energy change are

$$\Delta G^0_1 = -2FE_0(PQ/PQH_2) + 2RT\ln(10) \cdot pH_{lumen}, \tag{46}$$
$$\Delta G^0_2 = -FE_0(PC/PC^-), \tag{47}$$
$$\Delta G^0_3 = RT\ln(10)(pH_{stroma} - pH_{lumen}). \tag{48}$$

According to the stoichiometry (45), the overall standard Gibbs free energy change amounts to

$$\Delta G^0 = -\Delta G^0_1 + 2\Delta G^0_2 + 2\Delta G^0_3. \tag{49}$$

Finally, it is important to note that the *standard* redox potentials have to be used for the calculation. These are determined from the mid-point potentials E'^0 by (see [30])

$$E^0 = E'^0 + \frac{RT\ln(10)}{F} \cdot \Delta pH \cdot \frac{m}{n} = E'^0 + \frac{m}{n} \cdot 0.414\,V. \tag{50}$$

Similarly, all equilibrium constants were calculated from pairs of standard redox potentials. Table S2 specifies for each reaction which redox pairs were used for the determination of the equilibrium constant.

S6 Extending the model by qE-dependent quenching

To investigate how the system behaves if also a qE-dependent quenching mechanism is included, mimicking high-light adapted Chlamydomonas cells, we extend the model by

an additional differential equation simulating the state of a qE-dependent quencher. We here employ an extremely simple model, which assumes that the xanthophyll cycle is the only mechanistic cause for qE-dependent quenching. Although this is a crude simplification and does not exactly reflect the current hypotheses of NPQ mechanisms, it has been shown in [1] that reasonable agreement with experimental fluorescence measurements in Arabidopsis leaves can be obtained and that steady-state quenching levels can be accurately described. For Chlamydomonas acclimated to high light, the induced accumulation of LHCSR3 allows a strong qE component. For the present investigation, a simple mechanism that represents the fundamental principle that a low pH triggers energy-dependent quenching, is sufficient, because we are interested in the key differences between scenarios with or without qE-dependent quenching. A more detailed representation of the molecular mechanisms of the qE-component, such as proposed for higher plants in [4], will become necessary in future models, in particular to understand and predict the dynamics of quenching induction and relaxation. We expect that a future refinement of the model will also support to discriminate between alternative hypotheses regarding the precise mechanisms that induce NPQ.

Here, we assume that a quencher, corresponding to zeaxanthin and described in the model by the variable Q, is activated enzymatically by a process corresponding to the de-epoxidation of violaxanthin. This process is reversed by an enzymatic step corresponding to the expoxidation of zeaxanthin back to violaxanthin. The quencher variable Q assumes values between 0 and 1. Its dynamics are governed by the equation

$$\frac{dQ}{dt} = v_{\text{deep}} - v_{\text{epox}}, \tag{51}$$

where v_{deep} and v_{epox} describe the activities of quencher activation and de-activation, respectively. As in [1] and [4], we assume the de-epoxidase to be activated by a low lumenal pH and describe its dynamics by a Hill-type equation. The epoxidase is considered to be active constitutively.

$$v_{\text{epox}} = k_{\text{epox}}(1-Q)\frac{H^{n_{\text{Q}}}}{H^{n_{\text{Q}}} + {K_{\text{M,Q}}}^{n_{\text{Q}}}}, \tag{52}$$

$$v_{\text{deep}} = k_{\text{deep}}Q. \tag{53}$$

Activity of the quencher leads to a faster dissipation of energy as heat. Its effect is simulated by making the parameter k_H of the previous sections dynamic such that it becomes faster if the quencher is more active:

$$k_H = k_H^0 + Q \cdot k_H^{\text{dynamic}}. \tag{54}$$

The linear increase of the heat-dissipation rate with active quencher was adopted from [4]. However, it should be noted that no mechanistic evidence exists that any quencher, whatever its precise nature, should indeed lead to a linear increase in the heat-dissipation rate k_H. By modifying Eq. 54 other modes of activation can easily be reflected. Because changing the mechanism by which the quencher induced heat dissipation will result in different numerical values, as depicted for example in Fig. S3, modifying Eq. 54 provides a method to test different mechanistic hypotheses and validating these with systematically obtained experimental data.

References

[1] O. Ebenhöh, T. Houwaart, H. Lokstein, S. Schlede, K. Tirok, A minimal mathematical model of nonphotochemical quenching of chlorophyll fluorescence., Biosystems 103 (2) (2011) 196–204. doi:10.1016/j.biosystems.2010.10.011.
URL http://dx.doi.org/10.1016/j.biosystems.2010.10.011

[2] A. Laisk, H. Eichelmann, V. Oja, C3 photosynthesis in silico., Photosynth Res 90 (1) (2006) 45–66. doi:10.1007/s11120-006-9109-1.
URL http://dx.doi.org/10.1007/s11120-006-9109-1

[3] W. Liebermeister, E. Klipp, Bringing metabolic networks to life: convenience rate law and thermodynamic constraints., Theor Biol Med Model 3 (2006) 41. doi:10.1186/1742-4682-3-41.
URL http://dx.doi.org/10.1186/1742-4682-3-41

[4] J. Zaks, K. Amarnath, D. M. Kramer, K. K. Niyogi, G. R. Fleming, A kinetic model of rapidly reversible nonphotochemical quenching., Proc Natl Acad Sci U S A 109 (39) (2012) 15757–15762. doi:10.1073/pnas.1211017109.
URL http://dx.doi.org/10.1073/pnas.1211017109

[5] W. L. Butler, Energy distribution in the photochemical apparatus of photosynthesis, Annual Review of Plant Physiology 29 (1) (1978) 345–378. arXiv:http://www.annualreviews.org/doi/pdf/10.1146/annurev.pp.29.060178.002021, doi:10.1146/annurev.pp.29.060178.002021.
URL http://www.annualreviews.org/doi/abs/10.1146/annurev.pp.29.060178.002021

[6] H. Kirchhoff, U. Mukherjee, H.-J. Galla, Molecular architecture of the thylakoid membrane: lipid diffusion space for plastoquinone., Biochemistry 41 (15) (2002) 4872–4882.

[7] H. Böhme, Quantitative determination of ferredoxin, ferredoxin-nadp+ reductase and plastocyanin in spinach chloroplasts, European Journal of Biochemistry 83 (1) (1978) 137–141. doi:10.1111/j.1432-1033.1978.tb12077.x.
URL http://dx.doi.org/10.1111/j.1432-1033.1978.tb12077.x

[8] D. Heineke, B. Riens, H. Grosse, P. Hoferichter, U. Peter, U. I. Flügge, H. W. Heldt, Redox transfer across the inner chloroplast envelope membrane., Plant Physiol 95 (4) (1991) 1131–1137.

[9] M. A. Schöttler, H. Kirchhoff, E. Weis, The role of plastocyanin in the adjustment of the photosynthetic electron transport to the carbon metabolism in tobacco., Plant Physiol 136 (4) (2004) 4265–4274. doi:10.1104/pp.104.052324.
URL http://dx.doi.org/10.1104/pp.104.052324

[10] G. Finazzi, A. Furia, R. P. Barbagallo, G. Forti, State transitions, cyclic and linear electron transport and photophosphorylation in chlamydomonas reinhardtii., Biochim Biophys Acta 1413 (3) (1999) 117–129.

[11] N. Carrillo, E. A. Ceccarelli, Open questions in ferredoxin-nadp+ reductase catalytic mechanism., Eur J Biochem 270 (9) (2003) 1900–1915.

[12] K.-J. Dietz, U. Heber, Rate-limiting factors in leaf photosynthesis. i. carbon fluxes in the calvin cycle, Biochimica et Biophysica Acta (BBA) - Bioenergetics 767 (3) (1984) 432 – 443. doi:http://dx.doi.org/10.1016/0005-2728(84)90041-0.
URL http://www.sciencedirect.com/science/article/pii/0005272884900410

[13] J. Farah, F. Rappaport, Y. Choquet, P. Joliot, J. D. Rochaix, Isolation of a psaf-deficient mutant of chlamydomonas reinhardtii: efficient interaction of plastocyanin with the photosystem i reaction center is mediated by the psaf subunit., EMBO J 14 (20) (1995) 4976–4984.

[14] P. Q. Sétif, H. Bottin, Laser flash absorption spectroscopy study of ferredoxin reduction by photosystem i in synechocystis sp. pcc 6803: evidence for submicrosecond and microsecond kinetics., Biochemistry 33 (28) (1994) 8495–8504.

[15] R. de Wijn, H. J. van Gorkom, Kinetics of electron transfer from q(a) to q(b) in photosystem ii., Biochemistry 40 (39) (2001) 11912–11922.

[16] N. G. Bukhov, U. Heber, C. Wiese, V. A. Shuvalov, Energy dissipation in photosynthesis: Does the quenching of chlorophyll fluorescence originate from antenna complexes of photosystem ii or from the reaction center?, Planta 212 (2001) 749–758, 10.1007/s004250000486.
URL http://dx.doi.org/10.1007/s004250000486

[17] E. E. Pfundel, R. A. Dilley, The ph dependence of violaxanthin deepoxidation in isolated pea chloroplasts., Plant Physiol 101 (1) (1993) 65–71.

[18] A. Aliverti, T. Jansen, G. Zanetti, S. Ronchi, R. G. Herrmann, B. Curti, Expression in escherichia coli of ferredoxin:nadp+ reductase from spinach. bacterial synthesis of the holoflavoprotein and of an active enzyme form lacking the first 28 amino acid residues of the sequence., Eur J Biochem 191 (3) (1990) 551–555.

[19] M. Shin, Ferredoxin-nadp reductase from spinach, in: A. S. Pietro (Ed.), Photosynthesis and Nitrogen Part A, Vol. 23 of Methods in Enzymology, Academic Press, 1971, pp. 440 – 447. doi:DOI: 10.1016/S0076-6879(71)23116-5.
URL http://www.sciencedirect.com/science/article/B7CV2-4B7RF7H-GW/2/7a0df2d951f6a

[20] A. Aliverti, V. Pandini, G. Zanetti, Domain exchange between isoforms of ferredoxin-nadp+ reductase produces a functional enzyme., Biochim Biophys Acta 1696 (1) (2004) 93–101.

[21] A. Amunts, H. Toporik, A. Borovikova, N. Nelson, Structure determination and improved model of plant photosystem i., J Biol Chem 285 (5) (2010) 3478–3486. doi:10.1074/jbc.M109.072645.
URL http://dx.doi.org/10.1074/jbc.M109.072645

[22] B. Drop, M. Webber-Birungi, F. Fusetti, R. Kouřil, K. E. Redding, E. J. Boekema, R. Croce, Photosystem i of chlamydomonas reinhardtii contains nine light-harvesting complexes (lhca) located on one side of the core., J Biol Chem 286 (52) (2011) 44878–44887. doi:10.1074/jbc.M111.301101.
URL http://dx.doi.org/10.1074/jbc.M111.301101

[23] B. Drop, M. Webber-Birungi, S. K. N. Yadav, A. Filipowicz-Szymanska, F. Fusetti, E. J. Boekema, R. Croce, Light-harvesting complex ii (lhcii) and its supramolecular organization in chlamydomonas reinhardtii., Biochim Biophys Acta 1837 (1) (2013) 63–72. doi:10.1016/j.bbabio.2013.07.012.
URL http://dx.doi.org/10.1016/j.bbabio.2013.07.012

[24] S. I. Allakhverdiev, T. Tsuchiya, K. Watabe, A. Kojima, D. A. Los, T. Tomo, V. V. Klimov, M. Mimuro, Redox potentials of primary electron acceptor quinone molecule (qa)- and conserved energetics of photosystem ii in cyanobacteria with chlorophyll a and chlorophyll d., Proc Natl Acad Sci U S A 108 (19) (2011) 8054–8058. doi:10.1073/pnas.1100173108.
URL http://dx.doi.org/10.1073/pnas.1100173108

[25] S. Okayama, Redox potential of plastoquinone a in spinach chloroplasts., Biochim Biophys Acta 440 (2) (1976) 331–336.

[26] S. Suzuki, T. Sakurai, T. Nakajima, Characterization of plastocyanin isolated from brazilian elodea, Plant and Cell Physiology 28 (5) (1987) 825–831. arXiv:http://pcp.oxfordjournals.org/content/28/5/825.full.pdf+html.
URL http://pcp.oxfordjournals.org/content/28/5/825.abstract

[27] H. Witt, E. Bordignon, D. Carbonera, J. P. Dekker, N. Karapetyan, C. Teutloff, A. Webber, W. Lubitz, E. Schlodder, Species-specific differences of the spectroscopic properties of p700: analysis of the influence of non-conserved amino acid residues by site-directed mutagenesis of photosystem i from chlamydomonas reinhardtii., J Biol Chem 278 (47) (2003) 46760–46771. doi:10.1074/jbc.M304776200.
URL http://dx.doi.org/10.1074/jbc.M304776200

[28] M. C. Evans, P. Heathcote, Effects of glycerol on the redox properties of the electron acceptor complex in spinach photosystem i particles., Biochim Biophys Acta 590 (1) (1980) 89–96.

[29] R. Cammack, K. K. Rao, C. P. Bargeron, K. G. Hutson, P. W. Andrew, L. J. Rogers, Midpoint redox potentials of plant and algal ferredoxins., Biochem J 168 (2) (1977) 205–209.

[30] D. G. Nicholls, S. J. Ferguson, Bioenergetics, Academic Press, 1997.